Analysis of the Average Sampling Frequency for Level Crossing Analog-to-Digital Converters

Mengkun Ji, Keith M. Chugg
Ming Hsieh Department of Electrical and Computer Engineering
University of Southern California
Los Angeles, CA, USA 90089-2565
{mengkunj, chugg}@usc.edu

***Abstract*—This paper introduces two approaches to compute the average sampling frequency (ASF) of ideal level crossing analog-to-digital converters (LC-ADCs). The first is based on Rice's analysis method and can be used in various combinations of Gaussian signals. The second, a direct method, can only be used for narrowband modulated sinusoidal carrier input signals. These analysis results agree very well with computer simulations for ideal LC-ADCs and also highlight the oversampling issue for LC-ADCs (i.e., sampling at rates higher than Nyquist). Wu and Chen previously proposed a Gated LC-ADC to address this oversampling issue. We develop an approximate analysis for the ASF of this Gated LC-ADC by modeling the samples from the un-Gated LC-ADC as a Poisson arrival process. This approximation captures the desired effect of eliminating the oversampling issue reasonably well.**

***Index Terms*—Level crossing analog-to-digital converter (LC-ADC), average sampling frequency, level crossing rate.**

I. Introduction

Level crossing sampling (LCS) has been suggested as a method to adapt sampling rates in large bandwidth systems to the instantaneous frequency of the incoming signal [1]–[3]. For example, this method could be used to sense narrowband signals in a wideband of frequencies [4], [5], which has the potential to reduce much of the complexity and the power usage of tunable RF filters for narrowband selection [6]–[8]. There are some evidences that level crossing analog-to-digital converters (LC-ADCs) can adapt the sampling rate to the input signal bandwidth [9], [10]. In the development of LCS, Rice first proposed an analytic method to calculate the average single level crossing rate (LCR) for a zero mean, wide-sense stationary (WSS) Gaussian signal in [11] and applied this method for a sine wave plus random noise in [12]. Many researchers have since extended Rice's method to obtain the average single LCR for diverse scenarios [13]–[19]. In [13], [14], Adachi and Parsons applied Rice's method for time diversity reception in Rayleigh fading conditions. Patzold and Laue [15] extended the method for Rice fading channels. Dong and Beaulieu [16] employed the method for selection diversity. In [17], Abdi and Kaveh modified Rice's approach in terms of the characteristic function and applied it in a RAKE receiver. Yang and Alouini extended Rice's formula for generalized selection combining in [18] and for multiple independent random processes in [19]. However, currently neither analysis nor corresponding simulation of the average multi-level crossing rate exists for various signals, especially, for a narrowband signal plus broadband noise with some fixed signal-to-noise ratio (SNR), which is a common model for many communication and radar systems.

In this paper we develop expressions for the average sampling frequency (ASF) of ideal LC-ADCs. First, we extend Rice's approach to a multi-level crossing problem and apply it to various combinations of narrowband Gaussian signals and broadband Gaussian noise. Second, we use a direct approach to compute the ASF for a narrowband modulated sinusoidal carrier. These methods predict our computer simulation results well and also demonstrate the oversampling issue associated with LC-ADCs – i.e., sampling at a rate much higher than the Nyquist rate. To address the oversampling nature of LC-ADCs, Wu and Chen [20] proposed a modification that disabled sampling for a set period of time after a sample is latched. We analyze Gated LC-ADC using a Poisson arrival process to model the samples from the un-Gated LC-ADC. This approximate analysis predicts the simulation results reasonably well; it especially captures the desired effect of eliminating oversampling for the LC-ADC.

Additional motivation for the potential application of LC-ADCs in signal detection is discussed in Section II. In Section III, we develop the expressions for the ASF of LC-ADCs using Rice's method and the direct method. The ASF for various input signal models is computed using these methods and compared to numerical simulations in Section IV. The gated LC-ASF is analyzed in Section V. Section VI contains concluding remarks.

II. LC-ADC Motivation

For the wideband sensing system shown in Fig. 1, generally, there are two approaches to process incoming signals. The first approach is to use a tunable RF front-end to sequentially select each band of interest. Once a band is selected, it is digitized using a standard ADC at the Nyquist rate. Down-conversion can be achieved by either an analog mixer or direct down-conversion with the ADC. The drawback of this approach is that this RF front-end can be complex in circuit area and power.

This work was funded in part by the National Science Foundation (ECCS 1643004)

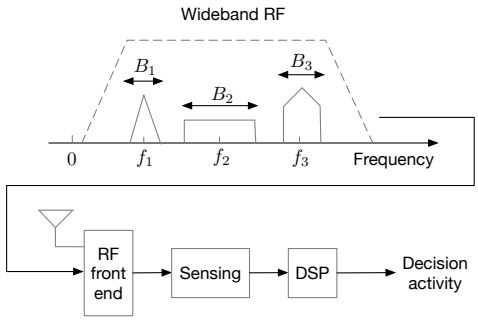

Fig. 1. Wideband sensing.

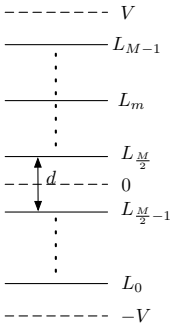

Fig. 2. Relationships among V, d and L_m in LC-ADC

The second approach is to use only a broadband (non-tunable) RF filter and then digitize the entire band. This could be done with a standard ADC (sampling at the Nyquist rate for the entire band) or a LC-ADC. Using a standard ADC may be prohibitively complex or exceed the current limits of technology; whereas using a LC-ADC has the potential to adapt the sampling rate to the instantaneous frequency occupancy [9], [10] therefore simplifying data conversion. In all cases, the samples of the output of the ADC would be processed using digital signal processing algorithms for the given task – e.g., signal detection and band activity. One challenge associated with using a LC-ADC is that the samples are non-uniform in time. Thus, either the samples must be interpolated to a uniformly sampled signal [21] or the DSP algorithms must be developed for the non-uniform samples – in either case a time quantizer is need to record the sample times. However, this is beyond the scope of this paper, which focuses on whether the LC-ADC can provide an advantage in terms of the sample rate relative to a conventional ADC.

III. ASF of Ideal LC-ADC

A. LC-ADC Modeling

The parameters that define an ideal LC-ADC model are shown in Fig. 2. The amplitude range of LC-ADC is $[-V, +V]$ and the bit resolution is q so that the total number of LC-ADC sampling levels is $M = 2^q$. The distance between levels is

$$d = \frac{2V}{M} = 2^{1-q}V. \tag{1}$$

and the m-th sampling level is

$$L_m = -V + \frac{d}{2} + md = [(2m+1)2^{-q} - 1]V, \tag{2}$$

where $m = 0, ..., M-1$. In the following sections, for random input signals, we scale the signal so that the clipping probability is 1%.

The model for an ideal LC-ADC is simple: every time the input signal crosses a level, in either the upward or downward direction, a sample is latched.

B. Rice's Method

A given ASF of an ideal LC-ADC for a signal is defined as the number of the times per second that the signal crosses the levels of the LC-ADC, in either positive or negative going direction. In [11], the average LCR of the level zero for a zero mean WSS Gaussian signal is expressed as

$$\mathrm{LCR}(0) = \frac{1}{\pi}\left[-\frac{R^{''}(0)}{R(0)}\right]^{1/2} = 2\left[\frac{\int_0^\infty f^2 S(f)df}{\int_0^\infty S(f)df}\right]^{1/2}, \tag{3}$$

where $R(\tau)$ is the auto-correlation function of the Gaussian signal and $R^{''}(\tau)$ is the second derivative of $R(\tau)$. The power spectral density (PSD) of the Gaussian signal is denoted as $S(f)$ and is the Fourier transform of $R(\tau)$. The average LCR of the level L_m for a zero mean WSS Gaussian signal is given by [11]

$$\mathrm{LCR}(L_m) = \exp\left(-\frac{L_m^2}{2R(0)}\right) \times \mathrm{LCR}(0). \tag{4}$$

Therefore, the ASF of a LC-ADC for a zero mean WSS Gaussian signal is

$$\bar{f}_s = \sum_{m=0}^{M-1} \mathrm{LCR}(L_m) = \mathrm{LCR}(0) \sum_{m=0}^{M-1} \exp\left(-\frac{L_m^2}{2R(0)}\right) \tag{5}$$

where M is the number of levels as shown in Fig. 2.

C. Direct Method for Modulated Sine Waves

1) Pure Sinusoid Case: To provide an intuitive sense of the ASF of a LC-ADC, in this subsection, we derive the ASF of LC-ADC for a pure sinusoid signal. We consider an input of the form $x(t) = A\cos(2\pi f_c t + \Theta)$, where $A \geq 0$, $f_c \geq 0$, and Θ are the amplitude, frequency, and phase of the sine wave. For this periodic input, the pattern of samples at the LC-ADC output will repeat each period. Thus, the ASF is the number of times that the sinusoid signal crosses the levels of LC-ADC within one period times the frequency f_c. In each period the sinusoid signal passes twice through all the sampling levels that it can reach. Hence, it follows that the ASF of LC-ADC for the sinusoid input is

$$\bar{f}_s(A) = \min\left\{4f_c\left[2^{q-1}\frac{A}{V}\right], 2^{q+1}f_c\right\}, \tag{6}$$

where the operator $[\cdot]$ rounds the value to the nearest integer. Note that the phase Θ does not affect the ASF and we have explicitly denoted the dependence on the amplitude A for further reference.

2) Narrowband Modulated Sinusoid Case: In the case of a narrowband modulated sine wave, the signal model is $x(t) = A(t)\cos(2\pi f_c t + \Theta(t))$, where the time-variation of $A(t)$ and $\Theta(t)$ is much slower than that of the carrier (i.e., this is the narrowband assumption). The amplitude and phase can be modeled as constant over one period, so that the expression in (6) can be averaged over the statistics of these parameters to obtain the ASF in the case of narrowband modulated sinusoids. In particular, since (6) does not depend on the phase, narrowband constant envelope modulation does not affect the ASF – i.e., this will have the same ASF as an unmodulated carrier. Similarly, for phase and amplitude modulation, only the amplitude modulation affects the ASF.

For a given period, the amplitude can be modeled as a constant, random level, $A(t) = A$, and the expression in (6) can be averaged over the statistics of the random variable A

$$\bar{f}_s = \int_0^\infty \bar{f}_s(a) f_A(a)\, da, \tag{7}$$

where $f_A(a)$ is the probability density function (pdf) of A.

The function $\bar{f}_s(A)$ has step discontinuities at the sampling levels L_m. Since A is non-negative, steps occur at $A = L_m$ for m ranging from $\frac{M}{2}$ to $M-1$. It follows that evaluating (7) is reduced to computing the probability that the amplitude is between a pair of non-negative levels, namely

$$p_0 = P\left(0 < A \le L_{\frac{M}{2}}\right) \tag{8a}$$

$$p_k = P\left(L_{\frac{M}{2}+k-1} < A \le L_{\frac{M}{2}+k}\right), \quad k = 1, \dots \frac{M}{2} - 1 \tag{8b}$$

$$p_{M/2} = P\left(L_{M-1} < A < \infty\right) \tag{8c}$$

Note that $\{p_k\}$ can be computed directly from the cumulative distribution function (cdf) of A, $F_A(a)$. For A in the range defining the event associated with p_k in (8), $\bar{f}_s(A) = 4kf_c$, which follows from (6). It follows that (7) is reduced to

$$\bar{f}_s = \sum_{k=0}^{\frac{M}{2}} p_k (4kf_c). \tag{9}$$

Two independent, zero mean Gaussian processes, each modulating an in-phase and a quadrature carrier, respectively, will lead to a Rayleigh distribution for the amplitude A. This is a reasonable approximation for high-order quadrature amplitude modulations (QAMs) or orthogonal frequency division multiplexing (OFDM) signals. In this case the cdf of A is

$$F_A(a) = 1 - \exp\left(-\frac{a^2}{2\sigma^2}\right), \; a \ge 0. \tag{10}$$

where σ^2 is the variance of each the in-phase and quadrature modulating signals. Once the loading convention from Section III-A is used to set σ, the values of p_k in (8) can be directly computed by using the cdf in (10).

IV. Numerical Experiments

In this section we compare the analysis results from Section III to computer simulations. For the purposes of evaluating the analysis based on Rice's method, we consider broadband and narrowband Gaussian processes to be the output of Butterworth filters when the input is a continuous time white Gaussian process. Specifically, to calculate Rice's ASF of LC-ADC, we represent the PSD of signals as

$$S(f) = \frac{G^2/2}{1 + \left(\frac{f - f_c}{f_{\text{cut}}}\right)^{2n}} + \frac{G^2/2}{1 + \left(\frac{f + f_c}{f_{\text{cut}}}\right)^{2n}}, \tag{11}$$

where G, n, f_c and f_{cut} are the DC gain, the order, the carrier frequency and the cutoff frequency, respectively. In all results that follow, $n = 2$ is used. To model broadband noise with bandwidth f_{cut}, $f_c = 0$ is used in (11), otherwise (11) models a narrowband (bandpass) process. We also consider narrowband Gaussian process in broadband Gaussian noise with PSD

$$S(f) = \text{SNR}_{\text{in-band}} \cdot S_s(f) + S_w(f), \tag{12}$$

where $\text{SNR}_{\text{in-band}}$ is the in-band signal-to-noise ratio (SNR) of this mixed Gaussian signal and $S_s(f)$ and $S_w(f)$ are the PSDs of the narrowband signal and the broadband noise, respectively. The analysis based on Rice's methods is obtained by using (11) in (3), numerically integrating it, and then following (4) and (5) to evaluate the final ASF in (5). The theoretical ASF obtained via the direct method is straightforward to calculate numerically.

To simulate on a digital computer, the inputs to the LC-ADC are modeled at an effective sampling rate of 10 THz for all numerical simulations in this paper. In these simulations, narrowband and broadband Gaussian signals are obtained by passing a zero mean, i.i.d. Gaussian sequence through the corresponding digital Butterworth filter that was obtained from (11) by using the bilinear transformation. To verify the direct method, in narrowband case, we pass two independent zero mean, i.i.d. Gaussian sequences through the corresponding digital low-pass Butterworth filter. The two filtered sequences are multiplied by in-phase and quadrature phase carrier waves, respectively. We use a 20 GHz bandwidth for the broadband noise and model a narrowband process as having bandwidth 20 MHz around $f_c = 5$ GHz.

The analysis based on Rice's method is compared with the corresponding simulations in Fig. 3 with excellent agreement. The ASF of a LC-ADC increases exponentially with the bit resolution q and is much higher than the corresponding Nyquist rates even when $q = 2$ – i.e., this is the over-sampling property of LC-ADCs. To determine a reasonable value for the in-band SNR, we can consider a signal detection problem or a digital communications problem. Since a detection problem may integrate over a longer time period, a digital communication system is expected to operate at a higher SNR than a signal detection system. The relationship between $\text{SNR}_{\text{in-band}}$ and E_b/N_0 for a digital communication system is $\text{SNR}_{\text{in-band}} = \eta \cdot E_b/N_0$, where η is the spectral efficiency. Assuming $\eta = 1$, as in Binary Phase Shift Keying (BPSK),

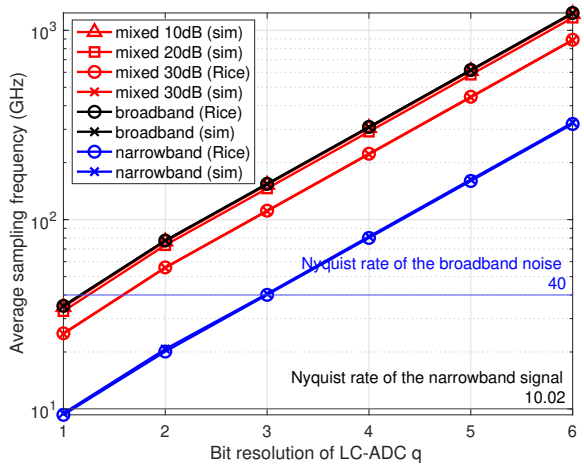

Fig. 3. Average sampling frequencies of LC-ADC for broadband Gaussian noise (with the cutoff frequency $f_{\text{cut}} = 20$ GHz), narrowband Gaussian signal (with the carrier frequency $f_c = 5$ GHz and the bandwidth $BW = 20$ MHz) and mixed Gaussian signals with various $\text{SNR}_{\text{in-band,dB}}$.

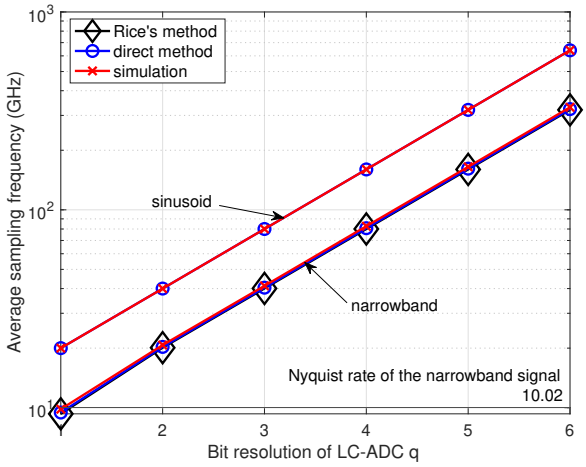

Fig. 4. Average sampling frequencies of LC-ADC for pure sinusoid signal (with 5 GHz frequency) and Rayleigh distributed narrowband signal (with the carrier frequency $f_c = 5$ GHz and the bandwidth $BW = 20$ MHz).

the uncoded bit error probability at $E_b/N_0 = 12$dB, is 10^{-8}. Thus, a value of $\text{SNR}_{\text{in-band}} = 12$dB may be considered a reasonably large SNR for a digital communication system or signal detection system. Inspecting Fig. 3, it is clear that, for a reasonable range of $\text{SNR}_{\text{in-band,dB}}$, the ASF of LC-ADC is mainly driven by the bandwidth of the noise, which is the bandwidth of the receiver front-end.

The theoretical curves for the direct method are shown to agree with the simulations in Fig. 4. Furthermore, Rice's method and the the direct method are both applied to a narrowband Gaussian modulating a sinusoidal carrier and provide excellent agreement, matching the simulations. Finally, we note that modulation of the carrier amplitude by a Rayleigh distributed amplitude causes a decrease in the ASF relative to that of an unmodulated carrier – i.e., this is because the modulated amplitude does not always cover the full range of the LC-ADC.

V. ASF of Gated LC-ADC

The gating mechanism proposed in [20] to address oversampling is illustrated in Fig. 5. Specifically, once a sample is latched, T_{out} seconds must pass before the next sample can be latched. This implies that the maximum sample rate for the Gated LC-ADC is $1/T_{\text{out}}$. We define $\{I_n\}_{n=0}^{\infty}$ as the consecutive sampling intervals after a reference LCS point (see Fig. 5) with the convention that $I_0 = 0$. Also, we define B_n as the event that n points are blocked or gated out – i.e., that the $(n+1)$-th point after the reference point is the first kept point under the gating mechanism. Letting $T_n = \sum_{k=0}^{n} I_k$, we can express the probability of B_n as

$$\begin{aligned} P(B_n) =& P\left(\{T_n < T_{\text{out}}\} \cap \{T_{n+1} \geq T_{\text{out}}\}\right) \\ =& P\left(T_n < T_{\text{out}}\right) \cdot P\left(T_{n+1} \geq T_{\text{out}} \middle| T_n < T_{\text{out}}\right). \end{aligned} \tag{13}$$

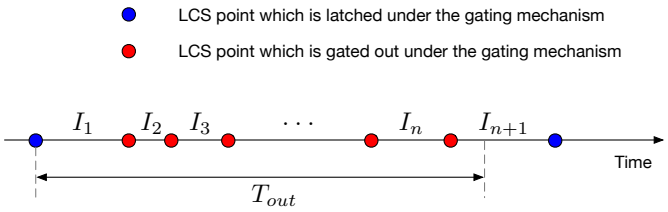

Fig. 5. Illustration of Gated LC-ADC mechanism with the event B_n occurring.

The events $\{B_n\}_{n=0}^{\infty}$ form a partition, and when B_n occurs, as illustrated in Fig. 5, the LC-ADC latches $(n+1)$ times as many samples as the Gated LC-ADC. Thus, the relationship between the ASF for these two LC-ADC variants is

$$\bar{f}_s = \left[\sum_{n=0}^{\infty}(n+1)P(B_n)\right] \bar{f}_{s,\text{gated}}. \tag{14}$$

To approximately compute $\bar{f}_{s,\text{gated}}$, we assume a Poisson arrival process for the LC-ADC samples, so that $\{I_n\}_{n=1}^{\infty}$ are i.i.d. exponential random variables with the rate parameter $\lambda = \bar{f}_s$. Hence, when $n \geq 1$, the random variable T_n is an Erlang distributed variable with the shape parameter equals n and the pdf of T_n is

$$p_{T_n}(\tau) = \begin{cases} \delta(\tau) & n = 0 \\ \frac{\lambda^n \tau^{n-1}}{(n-1)!} e^{-\lambda\tau} & n \geq 1 \end{cases} \tag{15}$$

where $\delta(\cdot)$ is the Dirac delta function. The complementary cdf of I_{n+1} is

$$P(I_{n+1} > \tau) = e^{-\lambda\tau}. \tag{16}$$

Using (15) and (16), we can express $P(B_n)$ in (13) as

$$P(B_n) = \int_0^{T_{\text{out}}} P(I_{n+1} > T_{\text{out}} - \tau | T_n = \tau) p_{T_n}(\tau) d\tau$$

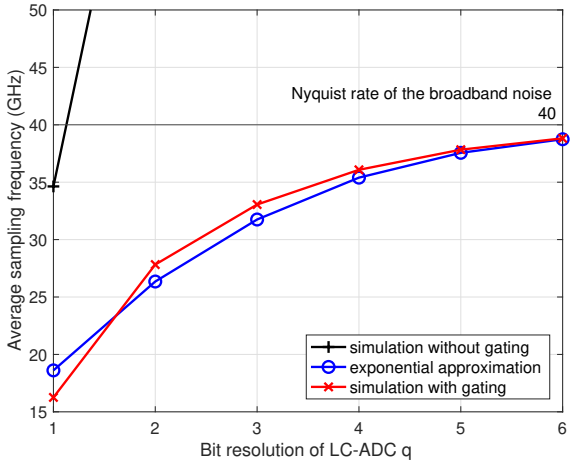

Fig. 6. Average sampling frequencies of LC-ADC with and without the gating; $T_{\text{out}} = \frac{1}{2f_{\text{cut}}}$ for broadband Gaussian with the cutoff frequency $f_{\text{cut}} = 20$ GHz.

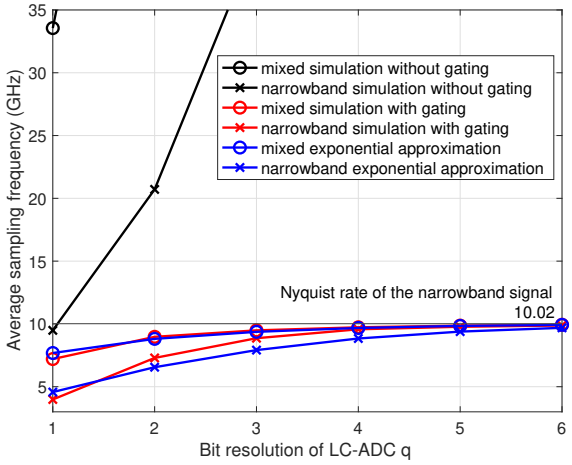

Fig. 7. Average sampling frequency of LC-ADC with and without the gating $T_{\text{out}} = \frac{1}{2(f_c+BW/2)}$ for narrowband Gaussian signal (with the carrier frequency $f_c = 5$ GHz and the bandwidth $BW = 20$ MHz) and mixed Gaussian, which is the narroband Gaussian signal plus broadband Gaussian noise (with the cutoff frequency $f_{\text{cut}} = 20$ GHz) with $\text{SNR}_{\text{in-band,dB}} = 20\text{dB}$ (a large reasonable in-band SNR).

$$= \int_0^{T_{\text{out}}} P(I_{n+1} > T_{\text{out}} - \tau) p_{T_n}(\tau) d\tau$$
$$= \frac{(\lambda T_{\text{out}})^n}{n!} \cdot e^{-\lambda T_{\text{out}}}. \quad (17)$$

Denoting $\lambda = \bar{f}_s$ and substituting (17) into (14), we can approximate $\bar{f}_{s,\text{gated}}$ as

$$\bar{f}_{s,\text{gated}} \approx \frac{\bar{f}_s \exp(\bar{f}_s T_{\text{out}})}{\sum_{n=0}^{\infty} \frac{(n+1)(\bar{f}_s T_{\text{out}})^n}{n!}}. \quad (18)$$

In our simulations, we set T_{out} to be equal to one over the corresponding Nyquist rate. In Figures 6 and 7, the exponential approximation curves match the corresponding simulations well. Comparing to the ASF simulations without gating, which increase exponentially with q, the ASF simulations with gating increase asymptotically to the corresponding Nyquist rates, respectively. The Gated LC-ADC can adjust the ASF by setting the value of T_{out} and exhibits some abilities to overcome the oversampling nature of LC-ADCs.

VI. Conclusion

In this paper, we adopted Rice's level crossing analysis to the ASF of a LC-ADC. We also developed a simple, direct method to analyze the ASF for narrowband modulated sine waves. These analysis results agree with computer simulations and also highlight the issue of oversampling associated with LC-ADCs. We also analyzed a previously proposed gated version of the LC-ADC using a Poisson arrival model for the LC-ADC samples. The results of our work indicate that even at reasonably high SNR, the broadband background noise will drive the sample rate for a LC-ADC and some mechanism, such as the gating mechanism, is required to limit the sampling frequency to below the Nyquist rate.

References

[1] N. Sayiner, H. V. Sorensen, and T. R. Viswanathan, "A level-crossing sampling scheme for A/D conversion," *IEEE Transactions on Circuits and Systems II: Analog and Digital Signal Processing*, vol. 43, no. 4, pp. 335–339, April 1996.

[2] K. Guan and A. C. Singer, "A level-crossing sampling scheme for both deterministic and stochastic non-bandlimited signals," in *2006 IEEE Sarnoff Symposium*, March 2006, pp. 1–3.

[3] ——, "A level-crossing sampling scheme for non-bandlimited signals," in *2006 IEEE International Conference on Acoustics Speech and Signal Processing Proceedings*, vol. 3, May 2006, pp. III–III.

[4] K. M. Guan and A. C. Singer, "Opportunistic sampling of bursty signals by level-crossing - an information theoretical approach," in *2007 41st Annual Conference on Information Sciences and Systems*, March 2007, pp. 701–707.

[5] C. Vezyrtzis and Y. Tsividis, "Processing of signals using level-crossing sampling," in *2009 IEEE International Symposium on Circuits and Systems*, May 2009, pp. 2293–2296.

[6] S. M. Qaisar, L. Fesquet, and M. Renaudin, "An improved quality filtering technique for time varying signals based on the level crossing sampling," in *2008 International Conference on Signals and Electronic Systems*, Sep. 2008, pp. 355–358.

[7] ——, "Computationally efficient adaptive rate sampling and filtering," in *2007 15th European Signal Processing Conference*, Sep. 2007, pp. 2139–2143.

[8] M. Malmirchegini, M. M. Kafashan, M. Ghassemian, and F. Marvasti, "Non-uniform sampling based on an adaptive level-crossing scheme," *IET Signal Processing*, vol. 9, no. 6, pp. 484–490, 2015.

[9] M. Greitans, "Processing of non-stationary signal using level-crossing sampling." 01 2006, pp. 170–177.

[10] M. Greitans, "Time-frequency representation based chirp-like signal analysis using multiple level crossings," in *2007 15th European Signal Processing Conference*, Sep. 2007, pp. 2254–2258.

[11] S. O. Rice, "Mathematical analysis of random noise," *The Bell System Technical Journal*, vol. 24, no. 1, pp. 46–156, 1945.

[12] ——, "Statistical properties of a sine wave plus random noise," *The Bell System Technical Journal*, vol. 27, no. 1, pp. 109–157, 1948.

[13] F. Adachi, M. T. Feeney, and J. D. Parsons, "Level crossing rate and average fade duration for time diversity reception in rayleigh fading conditions," *IEE Proceedings F - Communications, Radar and Signal Processing*, vol. 135, no. 6, pp. 501–506, 1988.

[14] ——, "Effects of correlated fading on level crossing rates and average fade durations with predetection diversity reception," *IEE Proceedings F - Communications, Radar and Signal Processing*, vol. 135, no. 1, pp. 11–17, 1988.
[15] M. Patzold and F. Laue, "Level-crossing rate and average duration of fades of deterministic simulation models for rice fading channels," *IEEE Transactions on Vehicular Technology*, vol. 48, no. 4, pp. 1121–1129, 1999.
[16] Xiaofei Dong and N. C. Beaulieu, "Average level crossing rate and average fade duration of selection diversity," *IEEE Communications Letters*, vol. 5, no. 10, pp. 396–398, 2001.
[17] A. Abdi and M. Kaveh, "Level crossing rate in terms of the characteristic function: a new approach for calculating the fading rate in diversity systems," *IEEE Transactions on Communications*, vol. 50, no. 9, pp. 1397–1400, 2002.
[18] Lin Yang and M. . Alouini, "Average level crossing rate and average outage duration of generalized selection combining," *IEEE Transactions on Communications*, vol. 51, no. 12, pp. 1997–2000, 2003.
[19] L. Yang and M. Alouini, "Level crossing rate over multiple independent random processes: an extension of the applicability of the rice formula," *IEEE Transactions on Wireless Communications*, vol. 6, no. 12, pp. 4280–4284, 2007.
[20] T. Wu and M. S. Chen, "A subranging-based nonuniform sampling adc with sampling event filtering," *IEEE Solid-State Circuits Letters*, vol. 1, no. 4, pp. 78–81, 2018.
[21] S. Maymon and A. V. Oppenheim, "Sinc interpolation of nonuniform samples," *IEEE Transactions on Signal Processing*, vol. 59, no. 10, pp. 4745–4758, 2011.